Conference Paper, Published Version

Kirca, V. S. Ozgur; Sumer, B. Mutlu

Sinking of Anchors and Other Subsea Structures due to Wave-Induced Seabed Liquefaction

Coastal Structures 2019 - Nils Goseberg, Torsten Schlurmann (eds) - © 2019 Bundesanstalt für Wasserbau
ISBN 978-3-939230-64-9 (Online) - DOI: 10.18451/978-3-939230-64-9_060

Sinking of Anchors and Other Subsea Structures due to Wave-Induced Seabed Liquefaction

V. S. Ozgur Kirca[1,2], B. Mutlu Sumer[1,3]
[1]*BM SUMER Consultancy & Research, Istanbul, Turkey*
[2]*Istanbul Technical University, Department of Civil Eng'g, Istanbul, Turkey*
[3]*Previously, Technical University of Denmark, Department of Mechanical Eng'g, Kgs. Lyngby, Denmark*

Abstract: This study presents an integrated modelling methodology, by which the sinking failure of Drag Embedment Anchors (DEA) as well as other subsea structures, such as gravity anchors and individual blocks, are modelled. The model has three components: (1) mathematical model for wave-induced residual liquefaction, (2) that for sinking of subsea structures, and (3) that for upward progression of compaction front in the post-liquefaction process, which presumably encapsulates the sinking structure, and therefore terminates the sinking. The present study demonstrates the implementation of the model with reference to three real-life subsea structures; a DEA, gravity anchors, and individual blocks. First, the details of the methodology are given. Then, a parametric study is presented for a series of soil, metocean, and anchor/block characteristics. Finally, remarks are made for practical applications of the methodology. The results of the study show that once the soil around the structure (DEA or block) liquefies, the structure immediately starts to sink. The sinking continues until the structure meets the compaction front. Sinking velocity for heavy structures such as the DEA is much larger than that of the compaction front, so that sinking terminates very close to the impermeable base of the soil column.

Keywords: Residual liquefaction; drag embedment anchors; gravity anchors; sinking of structures; permanent floating marine structures; floating offshore wind farms.

1 Introduction

Seabed soil, especially if it is in loose state and fine grained, may undergo a process termed as residual liquefaction as a result of seabed response to wave loading, especially if the soil is fine grained and loose. The cyclic shear deformations generated due to the alternating pressure variations exerted by the progressing waves on the seabed forces the soil grains to re-arrange at the expense of pore volume, which in turn pressurizes the pore-water (Sumer et al., 2006a; Sumer, 2014). If the accumulated pore-water pressure exceeds the initial mean normal effective stress (the quasi-isotropic stress that holds the soil particles), the seabed soil undergoes residual liquefaction, which reduces the bearing capacity of the soil to practically zero. When the seabed soil is liquefied, marine structures with large densities (gravity-based structures, steel pipelines, armor blocks, anchors, etc.) may sink into the seabed, while buried pipelines may float to the seabed if their specific gravity is less than that of the liquefied soil (such as gas pipelines). There are many such failure cases reported in the literature (Sumer, 2014).

Although the sinking damage/failure of structures on a liquefied seabed has been investigated in the last two decades (Sumer et al., 1999, Sumer and Fredsøe, 2002; Kirca, 2013; Sumer, 2014), none of these studies have addressed the behavior of anchors in a liquefied seabed in a comparative manner with other kinds of subsea structures. For vessels moored/anchored temporarily, sinking of the anchors as a result of wave-induced liquefaction may not constitute a practical problem since such a failure is the result of an extreme event. However, for permanent floating marine structures such as floating offshore wind turbines, sinking failure of the anchors due to residual liquefaction is a serious threat which should be accounted for in the design.

Floating storage and re-gasification units (FSRU), floating offshore oil and gas platforms, and floating offshore wind turbines (FOWT) are some of the most common floating permanent marine structures. Among these structures, FOWT has a particular and strategic importance as full-scale pilot floating offshore wind farms are being installed, or will be installed in the immediate future in great numbers. Since 80% of all the offshore wind resource is located in waters 60 m and deeper in European seas, FOWTs appear to be the preferred option in favor of bottom-fixed foundation alternatives. Considering that the total global installed power of offshore wind is foreseen to reach to some 520 GW by 2050, the strategic as well as commercial importance of FOWTs become significant (IRENA, 2018).

The anchoring systems are vital for FOWTs as well as other permanent floating marine structures, such that the limitation of anchor displacements is an important design criterion for the structure. Depending on the metocean conditions, water depth, and mooring line forces, different anchor types such as drag embedment anchors (DEA), gravity anchors, or suction caissons can be chosen for the anchoring alternative. Gravity anchors come up to be the most economical solution with their inexpensive production and installation, whereas DEA is usually the optimum choice, given their high holding capacity against lateral loads, and ease of installation. If the seabed soil experiences wave-induced liquefaction, DEAs would sink deeper than their design embedment, causing potential failure of the anchoring systems with multiple mooring legs. Furthermore, the holding capacity of the anchors may significantly decrease due to soil liquefaction during the liquefaction/compaction process, which may lead to the horizontal displacement of the anchors under mooring loads, and successive failure of the system. If there is a gravity anchor resting on liquefied soil, it would most likely undergo uncontrolled sinking, again potentially jeopardizing the stability of the floating structure.

In this study, an integrated modelling methodology is described, by which the sinking failure of a subsea structure, such as a DEA, a gravity anchor or an individual block, is modelled (Fig. 1). The model has three components: (1) mathematical model for wave-induced residual liquefaction, (2) that for sinking of subsea structures, and (3) that for upward progression of compaction front in the post-liquefaction process, which presumably encapsulates the sinking structure, and therefore terminates the sinking. The present study demonstrates the implementation of the model with reference to a selected DEA, a gravity anchor, and an individual block.

First, the details of the methodology are given, followed by a parametric study conducted for a series of soil, metocean, and anchor/block characteristics. Finally, remarks are made for practical applications of the methodology. An earlier version of this paper has been published in Kirca and Sumer (2019).

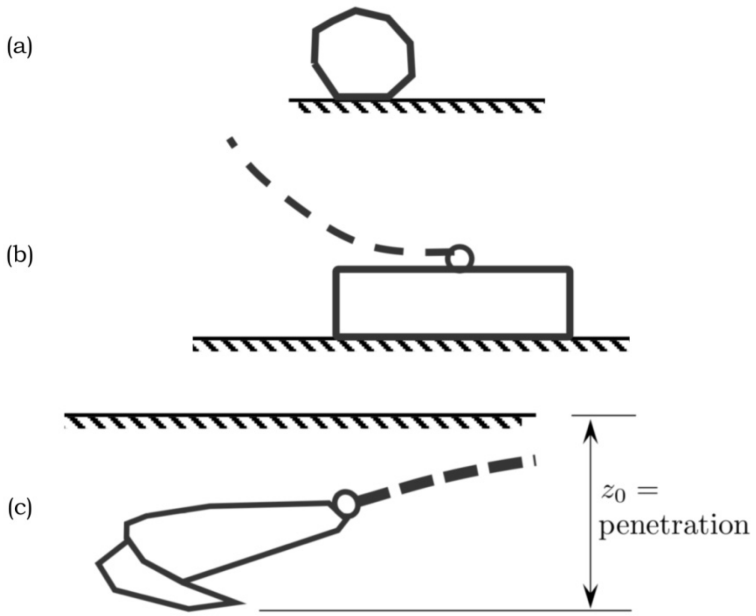

Fig. 1. Subsea structures considered in this study: (a) An individual block , (b) a gravity anchor, and (c) a drag embedment anchor DEA.

2 Methodology

2.1 Mathematical model for residual liquefaction

The first component of the integrated model is the mathematical model for residual liquefaction, which was first introduced by Sumer and Cheng (1999), and later validated in Sumer *et al.*'s (2012) against experiments reported in the same publication. The reader is referred to Sumer (2014, sec. 3.2) for a detailed description of the model with numerical examples. Only a brief summary of this model will be presented here for reasons of space.

Fig. 2 presents the definition sketch. The seabed soil is subject to a progressive wave with wave height H and wave period T. The conditions are such that the pore water pressure builds up under the cyclic action of the wave. Fig. 3 illustrates a schematic description of buildup of pore water pressure. A full description of these processes is given in Sumer et al. (2006a); see also Miyamoto et al. (2004). The pore water pressure builds up, and eventually attains a maximum value. When the period-averaged component of the accumulated pore pressure ($\bar{p}$) becomes equal to or greater than the initial mean normal effective stress (σ_0') the soil is said to be liquefied. The present mathematical model is concerned with this initial stage. The model comprises the following five elements: (1) Equation for accumulated pore-water pressure; (2) Source term; (3) Number of cycles to cause liquefaction; (4) Shear stress generated in the soil by the wave; and (5) Solution for the accumulated pore-water pressure. We note that the fourth element of the model involves the analytical solution of Hsu and Jeng (1994) for Biot's equations for the case of saturated, isotropic soil exposed to a progressive wave, which corresponds to the present case.

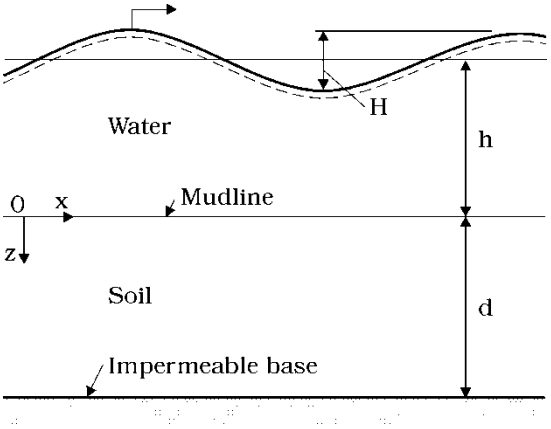

Fig. 2. Definition sketch for the mathematical model for residual liquefaction.

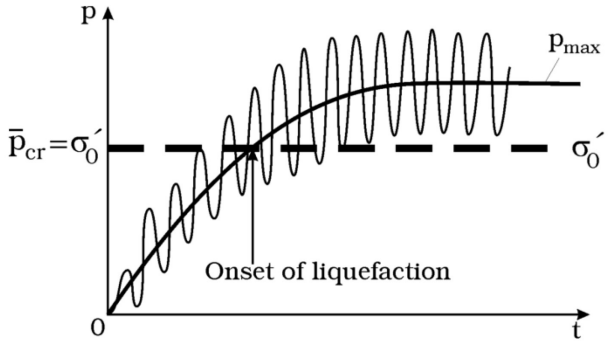

Fig. 3. Schematic description of buildup of pore pressure and resulting liquefaction (Sumer, 2014, p. 48).

Each of these elements are described in greater details in Sumer (2014, chp. 3) and Sumer et al. (2012), and the reader is referred to these publications. Briefly, given the wave properties (wave height, wave period, and the water depth), and the soil characteristics, the model solution returns (1) whether or not the soil is liquefied, and (2) the liquefaction depth z_L, if the soil is liquefied. The latter quantity may turn out to be equal to the soil depth d, if the soil is sufficiently shallow.

2.2 *Mathematical model for sinking of subsea structures in liquefied soil*

A typical new-generation DEA is composed a shank part (where mooring line is connected) and a fluke part which has a large surface area that gives the anchor a large holding capacity (maximum lateral load that can be borne by the anchor) when sufficiently dragged and embedded. For new-generation DEAs, the holding capacity can reach up to 50 times the anchors self-weight or even more (Turk Loydu, 2010). For reaching to the optimum holding capacity, DEA has an adjustable fluke angle, which is chosen to be larger for muddy soils, and narrower for sand or silt. These anchors are made of cast iron, which has a specific gravity around 7.5. The weight of an individual DEA may be between 1 ton and 65 tons. The new-generation DEAs with high holding capacity (such as Stevpris Mk6 model) are usually manufactured up to 30 tons.

A gravity anchor is basically a rectangular prism with a wide base area and relatively small height. Gravity anchors are usually manufactured from unreinforced concrete, with a specific gravity around 2.2 to 2.4.

An individual block, on the other hand, usually refers to an armor unit which may be rough angular quarry stone with a specific gravity of 2.65. Their nominal cubical diameters are typically $O(1)$ m.

When the soil is liquefied, it behaves like a very dense liquid composed of a mixture of soil grains and water, whose the specific gravity becomes around 1.8~2, depending on the initial soil specific gravity, and the coefficient of lateral earth pressure, Sumer et al. (2006b). If the seabed soil around a DEA embedded to an initial penetration depth of z_0 experiences residual liquefaction, the anchor will start to sink, given its large specific weight compared to the liquified soil. This is equally valid for a gravity anchor or an individual block resting on the seabed. The force-balance equation on this sinking DEA will be as follows (Sumer et al., 2006b; Kirca, 2013; Sumer, 2014):

$$W_A - V_A\, g\, \rho_{liq} = \frac{1}{2}\rho_{liq} C_D A_A {U_A}^2 \tag{1}$$

where W_A, V_A and A_A are the weight, volume and projection area of the subsea structure, respectively, ρ_{liq} is the density of the liquefied soil, g is the gravitational acceleration, C_D is the drag coefficient associated with the sinking of the DEA in liquefied soil, and U_A is the sinking velocity of the DEA. The left-hand side of Eq. (1) is the weight of DEA minus the buoyancy force (or pressure-gradient force) on the DEA. The right-hand side is the drag due to the sinking motion of the DEA in the liquefied soil.

Now, one might anticipate that C_D is a function of the sinking Reynolds number of the DEA in the liquefied soil, $Re_A = U_A D_A/\nu_{liq}$ (see e.g. the book of Sumer and Fredsøe (2006)). The term in the denominator is the kinematic viscosity of the liquefied soil, which is particularly cumbersome to determine. To circumvent this challenge, Sumer et al. (1999), and later Kirca (2013) and Sumer (2014) used the kinematic viscosity of water in the definition of the Reynolds number instead of that of the liquefied soil, and plotted the drag coefficient versus the Reynolds number based on their laboratory experiments. As the kinematic viscosity of liquefied soil remain practically unchanged in the laboratory and in the field, the empirical relation $C_D = f(Re)$ obtained in the laboratory (where Re is defined in terms of the water kinematic viscosity) can be used for field conditions as well without any problem. Therefore:

$$Re_A = \frac{U_A D_A}{\nu} \tag{2}$$

In Eq. (2), D_A is the representative size of the subsea structure, which can be expressed in terms of the projection area:

$$D_A = \sqrt{\frac{4\,A_A}{\pi}} \tag{3}$$

We note that D_A becomes nominal spherical diameter for an irregular block. The experimental findings of both Sumer et al. (1999) and Kirca (2013) suggested that the exact shape of the sinking object is of minor importance from the kinematics of sinking point of view. With reference to the experimental datasets of Kirca (2013) (cube, sphere and irregular shape blocks) and Sumer et al. (1999) (as re-analyzed by Sumer (2014)), the drag coefficient of the sinking subsea structure in the liquefied soil can be formulated in terms of the sinking Reynolds number regardless of its shape (DEA or otherwise) as follows:

$$C_D = max\left\{\frac{1.5\times10^6}{{Re_A}^{0.3}}; 3\times10^5\right\} \quad (4)$$

Here the value 3×10^5 is an asymptotic value corresponding to large Reynolds numbers.

The only unknown parameter yet to be calculated in Eq. (1) is the density of the liquefied soil, ρ_{liq}. For this, the model developed by Sumer et al. (2006b) (also reproduced in Sumer (2014, p. 193)) can be used. Accordingly, the concentration of liquefied soil, c, can be calculated by solving the equation given below:

$$(s-1) - [s(1-n)-1]\frac{(1+2k_0)}{3} - \frac{2}{2-3c}(1-c)^{2.697} - (s-1) = 0 \quad (5)$$

Here, s is the specific gravity of sediment grains, n is the porosity of the soil, and k_0 is the coefficient of lateral earth pressure. The density of the liquefied soil, ρ_{liq}, can be found from:

$$\rho_{liq} = \rho[(1-c) + c\,s] \quad (6)$$

where ρ is the density of water.

As such, the sinking velocity of DEA in liquefied soil, U_A, can be calculated via Eqs. (1) - (6).

2.3 Mathematical model for upward progression of compaction front

Once the soil is liquefied, it cannot remain in the liquefied state for larger times. Liquefaction is followed by the compaction process, which starts from the bottom of the liquefied soil column and progresses upwards. This process is described in greater details in Sumer et al. (2006a) and Sumer (2014, p. 53). Sinking of the subsea structure terminates when the anchor in its downward motion meets the compaction front (Sumer et al., 2010; Kirca, 2013; Sumer, 2014 p. 216). Fig. 4 illustrates this process.

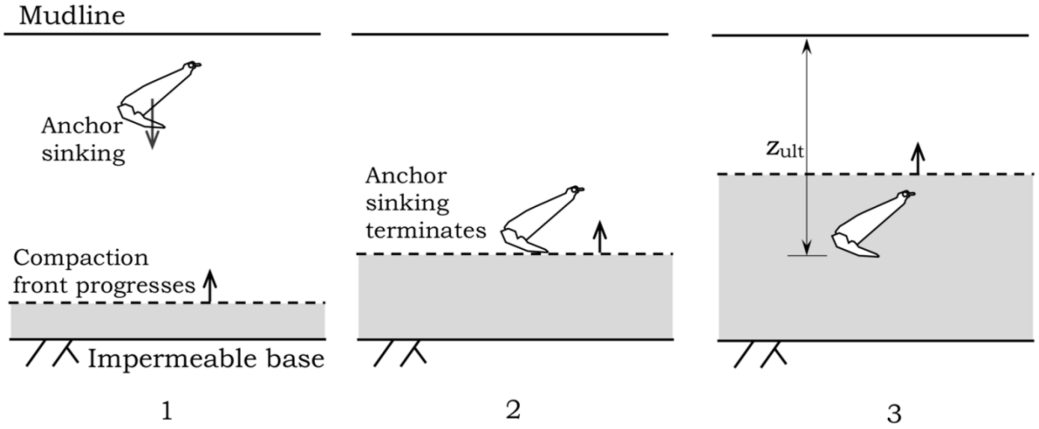

Fig. 4. Termination of sinking of an anchor in liquefied soil, due to the upward progression of the compaction front (adapted from Sumer, (2014, p. 218)).

Based on the physics of the compaction process, Sumer (2014, p. 107-113) developed a simple mathematical model, and validated it against experiments reported in Sumer et al. (2006b). With the latter model tested and validated, Sumer (2014) concluded that this simple model can be used for a quick assessment of the time scales associated with the compaction process. Sumer (2014, p. 110) gives the following expression for the compaction front velocity, U_c.

$$U_c = \frac{c}{1-n_1}(1-c)^{2.7}w_0 \quad (7)$$

Here $n_1$is the porosity of the compacted soil, and w_0 is the fall velocity of soil grains in clear water. As a first approximation, the porosity of the compacted soil can be related to the minimum void ratio of the sediment, such as $n_1 = e_{min}/(1+e_{min})$. Kirca (2013) used this approximation to compare Eq. (7) with his experimental data and found a good agreement. The fall velocity of the soil grains can be calculated via classical formulae given, e.g., in Fredsøe and Deigaard (1992, p. 198). To give the reader an idea, the progression velocity of compaction front generally appears to be within the range of $U_c = 1\times10^{-4}$~1×10^{-3} m/s.

3 Application of the model

A parametric study was conducted with the model described above for different types of subsea structures, wave properties and soil characteristics. Three different sizes of Stevpris Mk6 series DEAs are considered as given in Table 1. The projection area of the DEA given in Table 1 is calculated for the tilted fluke.

Tab. 1. DEA types and sizes that are used in the parametric study

Subsea Structure	Material	W_A (kN)	A_A (m^2)	D_n (m)	V_A (m^3)	z_0 (m)
DEA, Stevpris Mk6 - 6 ton	Cast iron	58.9	8.5	1.2	0.77	4
Gravity anchor	Concrete	4414.5	100.0	11.3	200.00	0
Individual armor block	Quartz	45.9	1.8	1.5	1.76	0

The wave characteristics used in the model runs are listed in Table 2. Sumer et al. (1999) showed that the characteristic wave height and period for irregular waves equivalent to the regular waves are the root-mean square wave height, H_{rms}, and zero-upcrossing wave period, T_z, respectively. Along with these wave characteristics, the return periods of the wave events are also noted in Table 2. The water depth was taken as $h = 60$ m. The last column of Table 2 shows the ratio of water depth to the deep-water wave length, L_0, which is calculated from linear wave theory. The storm duration (the duration during which the waves are effective) was taken as 5 hours for all wave conditions.

Tab. 2. Wave characteristics that are used in the parametric study

Return period (year)	H_{rms} (m)	T_z (s)	h (m)	h/L_0
25	4.5	9.8	60	0.400
50	5.5	10.7	60	0.336
100	6.5	11.9	60	0.272
250	7.3	12.5	60	0.246
500	9.0	13.8	60	0.202

The soil characteristics used for the model runs are given in Table 3. In this table, d is the soil depth, e_{min} and e_{max} are the minimum and maximum void ratios of the soil, D_r is the relative density defined as $D_r = (e_{max} - e)/(e_{max} - e_{min})$ and e being the void ratio, s is the specific gravity of soil grains, φ' is the angle of repose, k_0 is the coefficient of lateral earth pressure, ν_s is the Poisson ratio, G is the shear modulus of elasticity, k is the soil permeability, and d_{50} is the median grain size. As seen in Table 3, three of the parameters listed were changed parametrically to assess the sensitivity of sinking behavior of subsea structures to these parameters, namely, soil layer thickness d, relative density D_r, and median grain size d_{50}. Since the main concern of the present study is sinking of the structures rather than the initiation of wave-induced residual liquefaction, other parameters are kept constant during the model runs.

Tab. 3. Soil characteristics that are used in the parametric study

Parameter	Baseline Value	Range tested in the numerical runs
d (m)	7.5	5-10
D_r	0.35	0.25-0.50
d_{50} (mm)	0.07	0.05-0.12
e_{min}	0.6	N/A
e_{max}	1.2	N/A
s	2.65	N/A
φ'	38	N/A
k_0	0.384	N/A
ν_s	0.278	N/A
G (kPa)	10000	N/A
k (m/s)	0.00001	N/A

4 Results

In Fig. 5, the results of the mathematical model for residual liquefaction for the 100-year return period waves ($H_{rms} = 6.5$ m, $T_z = 11.9$ s), for the baseline values of the soil characteristics in Table 3 are presented as an example. The soil is liquefied if the accumulated period-averaged pore-water pressure value exceeds the initial mean normal effective stress, σ_0'. In non-dimensional form, this criterion is (Sumer, 2014, p. 47):

$$\frac{\bar{p}}{\sigma_0'} \geq 1 \tag{8}$$

Fig. 5 shows the variation of non-dimensional period-averaged pore-water pressure, $\bar{p}/\sigma_0'$, across the soil column for different times. It can be seen that the accumulated pore-water pressure exceeds the initial mean normal effective stress around $t = 11$ minutes at the mudline, meaning that liquefaction is initiated at $t = 11$ minutes. At $t = 23$ minutes, liquefaction reached to the impervious base, meaning that the entire soil column is liquefied. It should be noted that the model does not give liquefaction under wave conditions of 25 and 50-year return period waves listed in Table 2 for the baseline values in Table 3.

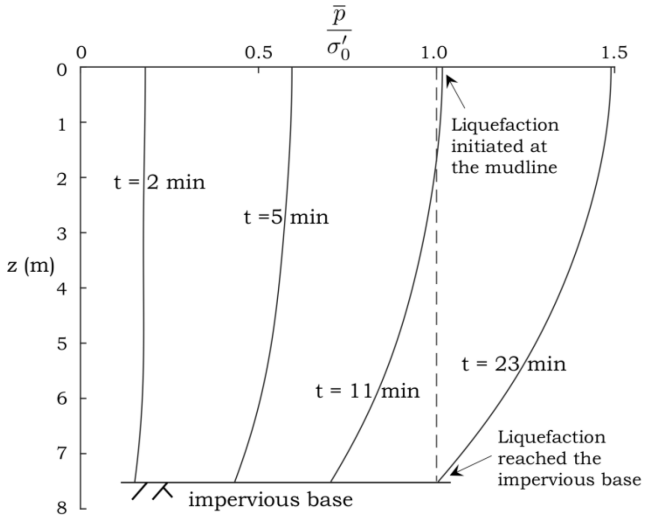

Fig.5. Results of an example with implementation of the mathematical model for residual liquefaction: variation of $\bar{p}/\sigma_0'$ vs. z for different times under 100-year return period waves ($H_{rms} = 6.5$ m, $T_z = 11.9$ s).

Typical result of the integrated mathematical model for the sinking of DEA is shown in Fig. 6, whereas similar results for gravity anchor and individual block are shown in Fig. 7. In these figures,

the sinking of structure is shown under 100-year return period waves, respectively, along with the progression of liquefaction and compaction front. As can be seen, the anchor starts to sink once the liquefaction arrives at $z = z_0$, and keeps sinking until it meets with the compaction front. The anchor motion reaches a steady state (in which the anchor moves with a practically constant velocity) shortly after the onset of sinking, and this continuous to be the case until the anchor meets the compaction front (Sumer et al., 1999; Kirca, 2013). The process is the same for gravity anchor and individual block cases, except that the latter subsea structures are resting on the seabed prior to sinking, and hence started to sink right after liquefaction started on the seabed. Not surprisingly, the ultimate sinking location is very close to the impervious base for all the three cases: $z_{ult} = 7.47$ m, $z_{ult} = 7.30$ m, and $z_{ult} = 7.33$ m, respectively for DEA, gravity anchor and individual block. This is due to the massive weight of the subsea structures modelled. One can see from Fig. 6 and 7 that the sinking velocities of all the three structures are not radically different. Although the DEA started to sink from penetration distance of $z_0 = 4$, the upward propagation velocity of the compaction front is so small compared to the sinking velocity of the subsea structures that gravity anchor and individual block was delayed as much as only 15 cm within a duration of 15 min.

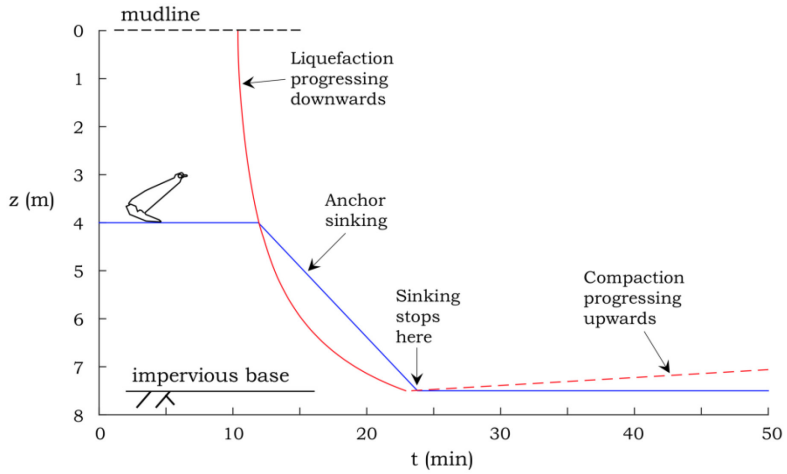

Fig.6. Results of the integrated model for sinking of Stevpris Mk6-6 ton DEA. 100-year return period waves ($H_{rms} = 6.5$ m, $T_z = 11.9$ s).

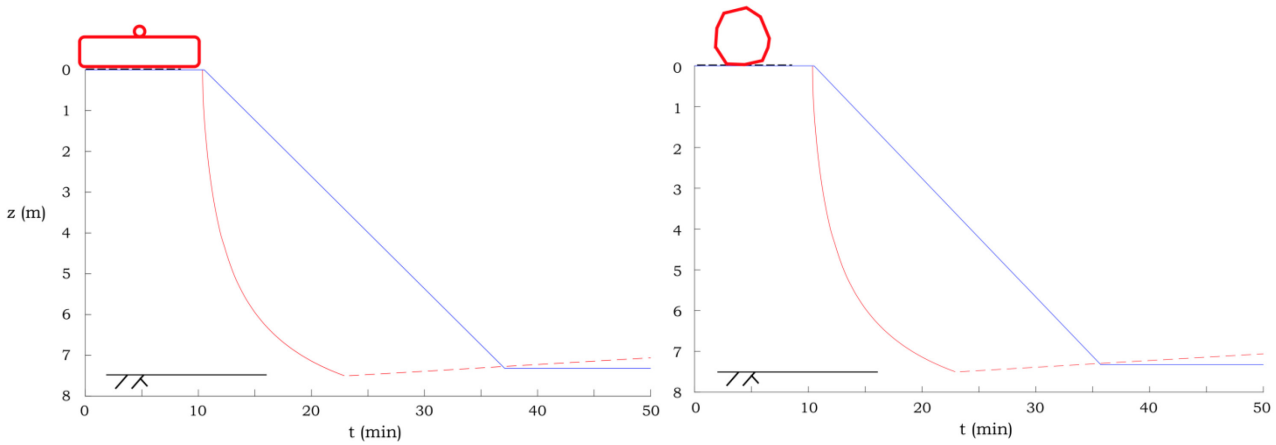

Fig.7. Results of the integrated model for sinking of Gravity anchor (left), and Individual block (right). 100-year return period waves ($H_{rms} = 6.5$ m, $T_z = 11.9$ s).

The model was also run for the three subsea structures under 250-year and 500-year return period waves given in Table 2. It was seen that the ultimate sinking location is very close to the impervious base regardless of the wave severity, provided that that waves are strong enough to liquefy the entire soil column. The results are not presented here for reasons of space.

The implementation of the methodology to find ultimate sinking depth, z_{ult}, the following procedure is to be followed:

1. Work out the time series of the liquefaction front progressing downwards, using the mathematical model for wave-induced residual liquefaction described in the preceding paragraphs, the first component of the present integrated model;
2. Likewise, work out the time series of the sinking of the DEA anchor, utilizing the mathematical model for sinking of DEA, the second component of the integrated model;
3. Also, work out the time series of the compaction front, using the mathematical for upward progression of compaction front, the third component of the integrated model; and
4. Finally, determine where and when the latter two time series meet, thereby determine the ultimate sinking depth of DEA, z_{ult}.

This exercise has been done for an extensive set of values of the quantities d (the soil depth), D_r (the relative density), and d_{50} (the grain size) (Table 3).

The results of the parametric study showed that once the seabed soil undergoes liquefaction sinking depth becomes non-zero. If the liquefaction is depth-limited (liquefaction depth z_L is smaller than the impervious base depth, $z_L < d$), the subsea structure sinks until the liquefaction depth, $z_{ult} \approx z_L$. If the entire soil column liquefies until the impervious base, then the sinking depth becomes very close to the impervious base depth, $z_{ult} \approx d$, for the case of DEA regardless of the tested values of soil parameters. For the gravity anchor and individual block, the resulting sinking depth becomes relatively less than the DEA, but not radically smaller.

5 Conclusion

An integrated mathematical model is described for the sinking failure of DEA type anchors, gravity anchors and other subsea structures in soils liquefied by waves. Sinking of anchors constitutes an important practical problem for the stability of floating offshore wind turbines (FOWT) and other permanent floating marine structures since it may lead to the failure of the entire structure.

The integrated model is composed of three parts; (1) initiation of residual liquefaction, (2) sinking of the anchor, and (3) termination of sinking as a result of upward progression of the compaction front. The implementation of the model is demonstrated by means of a parametric study conducted with different metocean, soil, and DEA characteristics. The following conclusions can be drawn:

- Once the soil around the structure liquefies, the structure starts to sink. The sinking continues until the sinking structure meets the compaction front. If the liquefaction does not reach the impermeable base (i.e. limited-depth liquefaction), then sinking terminates at the non-liquefied soil layer ($z_{ult} \approx z_L$).
- Given the heavy weight of the DEA, the upward progression velocity of compaction front is very small compared to the sinking velocity of the DEA ($U_c \ll U_A$). This is also valid for other tested subsea structures, namely gravity anchors and individual blocks. Consequently, the progression of the compaction front until it meets the sinking structure is usually very limited. Thus, in the case of liquefaction of the entire soil (full liquefaction), the ultimate sinking depth of heavy structures, such as DEA, becomes very close to the impermeable base ($z_{ult} \approx d$).
- The sinking depth of a subsea structure (individual block or DEA) is not correlated with the wave characteristics that causes liquefaction, provided that the soil is liquefied. In fact, when two wave cases which both causes full liquefaction are compared, more severe waves may even cause a slightly less sinking depth compared to relatively milder waves. This is because the liquefaction reaches to the impermeable base quicker, and consequently, the compaction front starts its upward progression quicker.

Finally, it is worth to mention that if the given method is to be applied to the case of seabed soil with cohesive fines (clay content), one can employ the model with using the characteristics of this mixed soil as input parameters, provided that the clay content is below a certain value (see Kirca et al., 2014 for further discussion of the subject).

Acknowledgement

This study was supported by The Scientific and Technological Research Council of Turkey (TUBITAK) through the research program TEYDEB-1507, Project No. 7170678.

References

Fredsøe, J., Deigaard, R. (1992) "Mechanics of coastal sediment transport", World Scientific, Singapore.

Hsu, J. R. C., Jeng, D.-S. (1994) "Wave-induced soil response in an unsaturated anisotropic seabed of finite thickness". International Journal for Numerical and Analytical Methods in Geomechanics, 18(11), 785-807.

Kirca, V. S. O. (2013) "Sinking of irregular shape blocks into marine seabed under wave-induced liquefaction", Coastal Engineering, 75, 40-51.

Kirca, V. S. O. and Sumer, B. M. (2018) "Sinking Failure of Drag Embedment Anchors Due to Wave-Induced Seabed Liquefaction", International Journal of Ocean and Coastal Engineering, 1(04), 1850006.

Kirca, V. S. O., Sumer, B. M., and Fredsøe, J. (2013) "Residual liquefaction of seabed under standing waves", ASCE Journal of Waterway, Port, Coastal, and Ocean Engineering, 139(6), 489-501.

Kirca, V. S. O., Sumer, B. M., and Fredsøe, J. (2014) "Influence of clay content on wave-induced liquefaction", ASCE Journal of Waterway, Port, Coastal, and Ocean Engineering, 140(6), 04014024.

IRENA (2018) "Offshore innovation widens renewable energy options", International Renewable Energy Agency, UAE http://www.irena.org/-/media/Files/IRENA/Agency/Publication/2018/Sep/IRENA_G7_offshore_wind_brief_2018.pdf

Miyamoto, J., Sassa, S. and Sekiguchi, H. (2004) "Progressive solidification of a liquefied sand layer during continued wave loading", Geotechnique, 54(10), 617–629.

Sumer, B.M. (2014) "Liquefaction around marine structures", World Scientific, Singapore. 978-981-4329-31-6.

Sumer, B.M. and Cheng, N-S. (1999) "A Random-Walk Model for Pore Pressure Accumulation in Marine Soils," Proc 9th Int Offshore and Polar Eng Conf, Brest, France, ISOPE, Vol 1, pp 521–526.

Sumer, B. M., Dixen, F. H., & Fredsøe, J. (2010) "Cover stones on liquefiable soil bed under waves", Coastal Engineering, 57(9), 864-873.

Sumer, B.M., Fredsøe, J., (2002) "The Mechanics of Scour in the Marine Environment", World Scientific, New Jersey, Singapore, London, Hong Kong.

Sumer, B. M., Fredsøe, J., (2006) "Hydrodynamics around cylindrical structures", Revised Ed. World Scientific, Singapore.

Sumer, B.M., Fredsøe, J., Christensen, S., Lind, M.T. (1999) "Sinking/floatation of pipelines and other objects in liquefied soil under waves", Coastal Engineering, 38, 53–90.

Sumer, B.M., Hatipoglu, F., Fredsøe, J., Sumer, K (2006a) "The sequence of sediment behaviour during wave-induced liquefaction", Sedimentology, 53, 611–629.

Sumer, B. M., Hatipoglu, F., Fredsøe, J., & Hansen, N. E. O. (2006b) "Critical flotation density of pipelines in soils liquefied by waves and density of liquefied soils", Journal of waterway, port, coastal, and ocean engineering, 132(4), 252-265.

Sumer, B.M., Kirca, V.S.O., Fredsøe, J. (2012) "Experimental validation of a mathematical model for seabed liquefaction under waves", Int. J. Offshore and Polar Eng. 22 (2), 133–141.

Turk Loydu (2010) "Multi-Point Mooring Systems", Specification Chapter-70, Turk Loydu, Istanbul, Turkey. http://www.turkloydu.org/pdf-files/turk-loydu-kurallari/cilt-d/chapter-70-multi-mooring-systems-2010.pdf